Pharmacogn. Mag.
A multifaceted peer reviewed journal in the field of Pharmacognosy and Natural Products
www.phcog.com | www.phcog.net

ORIGINAL ARTICLE

Angelica gigas Nakai Attenuated Inflammatory Response on Monosodium Iodoacetate-Induced Osteoarthritis

Jin A. Lee, Min Ju Kim, Mi-Rae Shin, Hae-Jin Park[1], Seong-Soo Roh

Department of Herbology, Korean Medicine of College, Daegu Haany University, Suseong-gu, Deagu, [1]DHU Bio Convergence Testing Center, 1 Hanuidae-ro, Gyeongsan 38610, Korea

Submitted: 08-Oct-2020 Revised: 23-Mar-2021 Accepted: 13-May-2021 Published: 19-Sep-2022

ABSTRACT

Background: *Angelica gigas* Nakai (AGN) is well-known for anti-inflammatory and anti-oxidative effects; however, the mechanism underlying the protective effects of AGN on monosodium iodoacetate (MIA)-induced osteoarthritis (OA) remains unknown. **Objectives:** Our objectives of this study were to evaluate the anti-inflammatory effect of AGN on MIA-induced OA and investigate the potential mechanism which underlies such effect. **Materials and Methods:** The dried herb AGN was extracted with distilled water. After the experiment was conducted for 4 weeks using 7-week-old male Sprague–Dawley rat. AGN (200 mg/kg body weight/day) was orally administered for 14 days from day 7 after intra-articular injection of MIA (50 μL with 80 mg/mL), and the effects were compared with those of MIA-treated control group. We examined the weight-bearing ability of hind paws, biomarkers related to oxidative stress in cartilaginous tissue. In addition, various factors associated with inflammatory and cartilage degeneration in cartilaginous tissue detected by the Western blot analysis. **Results:** Our results from an *in vivo* model of OA indicate that AGN inhibits inflammatory factors such as inducible nitric oxide synthase, cyclooxygenase-2, tumor necrosis factor-α, interleukin-6 (IL-6), and IL-1β via nuclear factor kappa B signaling pathway. AGN suppresses the expression of matrix metalloproteinase, proteolytic enzyme, and also elevates tissue inhibitor of metalloproteinase which inhibited degradation of the extracellular matrix. Moreover, antioxidant defense was enhanced through the nuclear factor erythroid 2-related factor 2/heme oxygenase-1 pathway. **Conclusion:** Taken together, these results demonstrate the effectiveness of AGN at the inflammation associated with joint disorders. Our results also suggest that AGN could serve as a potential candidate for alternative therapeutic treatment of OA.

Key words: *Angelica gigas* Nakai, anti-inflammatory, antioxidant, monosodium iodoacetate, osteoarthritis

SUMMARY

- *Angelica gigas* Nakai (AGN) is well-known for anti-inflammatory and anti-oxidative effects. Our objectives of this study were to evaluate the anti-inflammatory effect of AGN on monosodium iodoacetate (MIA)-induced osteoarthritis (OA). As a result of the experiment, it was confirmed that AGN suppressed excessive ROS in osteoarthritis and increased the antioxidant effect through Nrf2/HO-1. Moreover, AGN could inhibit the expression of inflammation factors by NF-κB inactivation. Our results suggest that AGN could serve as a potential candidate for alternative therapeutic treatment of OA.

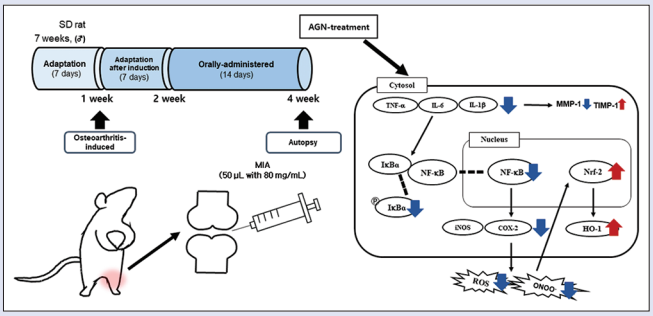

Abbreviations Used: AGN: *Angelica gigas* Nakai; MIA: Monosodium Iodoactate; OA: Osteoarthritis; Indo: Indomethacin; HWBD: Hindpaw weight bearing distribution; ROS: Reactive oxygen species; ONOO-: Peroxynitrite; Nrf2: Nuclear factor erythroid 2 related factor 2; HO-1: Heme oxygenase 1; MMPs: Matrix metalloproteinases; TIMPs: Tissue inhibitor of metalloproteinases; NF-κBp65: Nuclear factor kappa B p65; IκBα: Inhibitor of κB.

Correspondence:

Prof. Seong Soo Roh,
Department of Herbology, Korean Medicine of College, DaeguHaany University, 136, Shinchendong–ro, Suseong-gu, Deagu 42158, Republic of Korea.
E-mail: ddede@dhu.ac.kr

DOI: 10.4103/pm.pm_422_20

Access this article online
Website: www.phcog.com
Quick Response Code:

INTRODUCTION

Osteoarthritis (OA) is one of chronic arthritis characterized by inflammation and cartilage degradation. OA causes physical limitations, mental stress, socio-economic burden, and disability.[1,2] It has been acknowledged through many studies that the cause of OA is related to inflammation. Therefore, anti-inflammatory drugs such as nonsteroidal anti-inflammatory drugs (NSAIDs) are used to relieve OA symptoms. However, these drugs cannot delay the progression of OA and it just relieves the pain. Hence, new strategies for its delay are urgently needed.[3]

Many studies have shown iinflammatory cytokines including interleukin (IL)-1 β and tumor necrosis factor (TNF)-α are important factors in OA pathogenesis,[4-6] which is intimately related to cartilage matrix degradation. Matrix metalloproteinases (MMPs), proteolytic enzyme, is another factor closely associated with the degradation of cartilage matrix, and both interleukin-1 (IL-1) β and TNF-α can up-regulate MMPs expression.[7-10] Moreover, IL-1 β-induced nuclear factor kappa B (NF-κB) plays a central role in the expression of several inflammatory factors known as the pathogenesis of OA. Activated NF-κB

Cite this article as: Lee JA, Kim MJ, Shin MR, Park HJ, Roh SS. *Angelica gigas* Nakai attenuated inflammatory response on monosodium iodoacetate-induced osteoarthritis. Phcog Mag 2022;18:783-9.

can trigger extracellular matrix (ECM) degradation products, leading to OA.[11,12] Hence, the inhibition of inflammation may be a valid approach for the improvement of OA.

Angelica gigas Nakai (AGN) (local name dang-gui), traditional herbal medicinal plant in Korea, is mainly used for the treatment of menopausal syndromes.[13] Its pyranocoumarin compounds, such as decursin, decursinol angelate (DA), nodakenin, and demethylsuberosin, exert varying pharmacological effects.[14,15] Especially, both decursin and DA have been reported to exhibit anti-inflammatory effects.[16-19]

The purpose of our study was to elucidate reveals the mechanism for AGN to reveal relief of inflammation and protection of ECM through inhibition of NF-κB activation in the monosodium iodoacetate (MIA)-induced OA model.

MATERIALS AND METHODS

Materials

MIA, phenylmethylsulfonyl fluoride (PMSF), and dithiothreitol (DTT), diethylenetriaminepenta-acetic acid (DTPA) and dihydrorhoda mine 123 (DHR 123) were purchased from Sigma Aldrich Co., Ltd (St. Louis, MO, USA). The protease inhibitor mixture solution and ethylenediaminetetraacetic acid (EDTA) were purchased from Wako Pure Chemical Industries, Ltd., (Osaka, Japan). 2',7'-Dichlorofluorescein diacetate (DCF-DA) was obtained from Molecular Probes (Eugene, OR, USA). ECL Western blotting detection reagents and pure nitrocellulose membranes were supplied by GE Healthcare (Piscataway, NJ, USA). 0.3 mL-insulin syringe was obtained from BD Medical-Diabetes Care (Holdrege, USA). Besides, all other chemicals and reagents were purchased from Sigma Aldrich Co., Ltd., (St Louis, MO, USA).

Preparation of *Angelica gigas* Nakai extract

AGN was purchased as a dried herb from Bonchowon (Yeoungcheon, Korea), in 2018. The plant materials were authenticated by Professor SS Roh at College of Korean Medicine at Daegu Haany University. The dried herb AGN (300 g) was extracted with distilled water (3 L) for 2 h (DW-790, Daewoongbio, Chungbuk, Korea). After filtration (285 mm), the solution was evaporated under reduced pressure (N-1100, Eyela, Tokyo, Japan) and then freeze dried (FD5508, IlShin, Seoul, Korea) to provide an extract with a yield of 27.1% by weight of the starting materials (number of the plant material; 2019-34). The concentrate was lyophilized and subsequently stored at −20°C until use.

Angelica gigas Nakai analysis by high-performance liquid chromatography chromatogram

The extract of AGN (10 mg) was dissolved in 1 mL of methanol. 10 µL of sample was injected into high-performance liquid chromatography (HPLC) using ZORBAX Eclipse XDB-C_{18} (4.6 mm × 150 mm; particle size 5 µm, [Agilent Technologies, Inc., USA]). The mobile phase was composed of MeOH (A) and water (B). The elution conditions were as follows: the initial mobile phase of 20% A and 80% B was held for 0 min; a gradient was the napplied to 70% A and 30% B for 30 min; 70% A and 30% B for 50 min wash with 100% B. The column temperature was kept at a constant 25°C throughout the analysis, with a flow rate of 2.0 mL/min and an injection volume of 10 mg/mL in 50% of Methanol. Identification was based on the comparisons of retention time sand UV spectra with those of commercial standards. Quantitation was performed based on external standards, with a mixture of standards of known concentration analyzed in duplicate before and after each batch of samples. The peak areas were used to calculate the sample contents of the compounds. The components of major compounds (Nodakenin, Demethylsuberosin, Decursin, and Decusinol angelate) were detected from AGN. The measurement was repeated three times for each sample. Representative HPLC results are illustrated in Figure 1

. The amount was as follows: AGN: 8,902 µg/g Nodakenin, 6,650 µg/g Demethylsuberosin, 35,065 µg/g Decursin and Decusinol angelate.

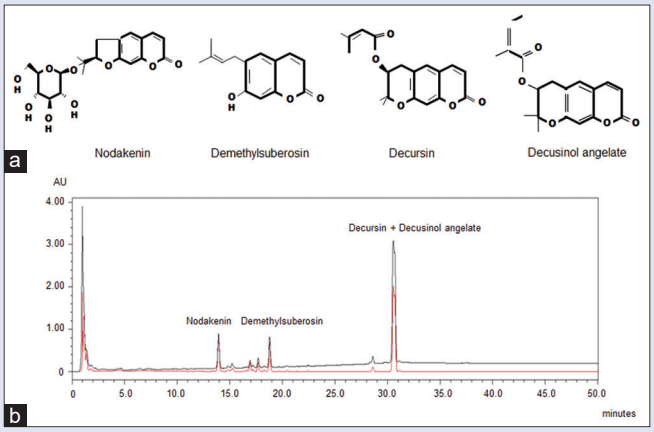

Figure 1: High performance liquid chromatography profile of *Angelica gigas* Nakai. (a) Chemical structure of Nodakenin, Demethylsuberosin, Decursin, and Decusinol angelate, (b) HPLC chromatogram of the extract of *Angelica gigas* Nakai

Development of osteoarthritis with monosodium iodoacetate injections and *Angelica gigas* Nakai administration

Seven-week-old male Sprague–Dawley rat weighing 200–250 g at the start of the experiment was purchased from DBL Co. (Eumseong, South Korea). The animals were housed three per cage in a room with controlled temperature conditions (23°C ± 2°C), humidity (about 55 ± 5%), and lighting (12 h light/dark cycle) with access to freely food and water. All animal procedures were approved by the Animal Research Ethics Committee of the Daegu Haany University (Permit Number: DHU2019-047). After adaptation (1 week), rats are randomly arranged in the descending order of weight and assigned into four groups of equal number (n = 8) without statistical significance among the groups. Group 1 included the normal rats (Normal). Group 2 included the MIA control rats (Control). Group 3 included the Indomethacin 5 mg/kg-administered and MIA rats (Indo). Group 4 included the AGN 200 mg/kg-administered and MIA rats (AGN). The normal and MIA control rat groups were administrated water using a stomach tube, whereas the other groups were orally administered Indomethacin 5 mg/kg or AGN 200 mg/kg using a stomach tube for 2 weeks. OA was induced in SD rats employed the method of Wang *et al.* with minor modification.[20] After anesthetization with injection of zoletil mixture (Vibrac, France) 0.75 mg/kg intraperitoneally, rats were injected with MIA 80 mg/kg in a 50 µL volume using a 0.3 mL-insulin syringe (31G needle) inserted through the patellar ligament into the intra-articular space of the right knee; normal rats were injected with an equivalent volume of saline. The rats in all groups were sacrificed after the end of the experimental period. The rats were anesthetized using a mixture of zoletil and xylazine and euthanized by isoflurane overdose. The entire joint was removed immediately and frozen in liquid nitrogen. Blood was drawn from the abdominal vein using a 10 mL syringe, centrifuged at 3,000 rpm for 20 min at 4°C, and serum collected and stored at −80°C until analysis.

Measurements of hind paw weight-bearing distribution

Weight bearing was assessed using an in capacitance meter that measures the distribution of weight bearing across each hind limb. The balance in the weight-bearing capability of the hindpaws was disrupted after OA induction. A significant shift in weight from the arthritic site to the contralateral limb, i.e. a weight-bearing deficit, was considered to be an index of pain. Inflammatory pain was measured via the weight bearing of the paw load using Incapacitance Meter Apparatus (IITC Life Science Inc., CA, USA).[21] The weight distribution ratio was calculated using the following equation:

$$\text{Weight distribution ratio} = \frac{\text{Weight on left hind limb}}{\text{Weight on right hind limb}} \times 100$$

Measurement of reactive oxygen species level in cartilaginous tissue

The reactive oxygen species (ROS) levels were measured by employing the method of Ali *et al.*[22] 25 mM DCF-DA was added to cartilaginous tissue. After incubation for 30 min, the changes in fluorescence values were determined at an excitation wavelength of 486 nm and emission wavelength of 530 nm using a microplate fluorescence reader, model infinite M200 PRO (Tecan, Austria).

Measurement of $ONOO^-$ Level in cartilaginous tissue

The peroxynitrite ($ONOO^-$) level was assessed by a modified Kooy's method with minor modifications,[23] which involves the monitoring of highly fluorescent rhodamine 123, which is rapidly produced from non-fluorescent dihydrorhodamine (DHR) 123 in the presence of $ONOO^-$. Moreover, its final fluorescent intensities remained unchanged over time. Cartilaginous tissue was added to the rhodamine buffer. In brief, the rhodamine buffer (pH 7.4) consisted of 50 mM sodium phosphate dibasic, 50 mM sodium phosphate monobasic, 90 mM sodium chloride, 5 mM potassium chloride and 5 mM diethylenetriamine penta-acetic acid. The final DHR 123 concentration was 5.0 μM. Five minutes after treating with or without the addition of authentic $ONOO^-$, the background and final fluorescent intensities of the samples were measured. The assay buffer was prepared prior to use and placed on ice. The fluorescence intensity of the oxidized DHR 123 was measured with a microplate fluorescence reader, model infinite M200 PRO (Tecan, Austria), at 485 nm excitation and 535 nm emission. The results were expressed as the inhibition level of oxidation of DHR 123 and calculated from the final fluorescence intensity minus background fluorescence intensity.

Preparation of cytosol and nuclear fractions

Protein extraction was performed according to the method of Komatsu with minor modifications.[24] Cartilaginous tissue for cytosol fraction was homogenized with ice-cold lysis buffer A (250 mL) containing 10 mM HEPES (pH 7.8), 10 mM KCl, 2 mM $MgCl_2$, 1 mM DTT, 0.1 mM EDTA, 0.1 mM PMSF and 1,250 μL protease inhibitor mixture solution. The homogenate incubated at 4°C for 20 min. And then 10% NP-40 was added and mixed well. After centrifugation (12,000 rpm for 2 min at 4°C) using Eppendorf 5415R (Hamburg, Germany), the supernatant liquid (cytosol fraction) was separated new e-tube. The left pellets were washed twice by buffer A and the supernatant was discarded. Next, the pellets were suspended with lysis buffer C (20 mL) containing 50 mM HEPES (pH 7.8), 50 mM KCl, 300 mM NaCl, 1 mM DTT, 0.1 mM EDTA, 0.1 mM PMSF, 1% (v/v) glycerol, and 100 μL protease inhibitor mixture solution suspended and incubated at 4°C for 30 min. After centrifugation (12,000 rpm for 10 min at 4°C), the nuclear fraction was prepared to collect the supernatant. The protein concentration was determined using BCA Protein Assays by Thermo Fisher Scientific (Waltham, USA). Both cytosol and nuclear fractions were kept at-80°C before the analysis.

Immunoblotting analysis

For the estimation of nuclear factor erythroid 2-related factor 2 (Nrf2), NF-κBp65 and histone (1:1000; Santa Cruz Biotechnology, Dallas, TX, USA) 10 μg of proteins from each nuclear fraction were electrophoresed through 8%–10% sodium dodecyl sulfate polyacrylamide gel (SDS-PAGE). Separated proteins were transferred to a nitrocellulose membrane, blocked with 5% (w/v) skim milk solution for 1 h, then incubated with primary antibodies to Nrf2, NF-κBp65 and histone, respectively, overnight at 4°C. After the blots were washed, they were incubated with anti-rabbit or anti-mouse immunoglobulin G HRP-conjugated secondary antibody (1:3000; Santa Cruz Biotechnology) for 1.5 h at the room temperature. In addition, 10–12 μg proteins of each cytosol fraction were electrophoresed 10%–14% sodium dodecylsulfate polyacrylamide gel (SDS-PAGE) for immunodetection of p-IκBα/cyclooxygenase-2 (COX-2)/inducible nitric oxide synthase (iNOS)/TNF-α/IL-6/IL-1β/heme oxygenase-1 (HO-1)/MMP-1/tissue inhibitor of metalloproteinase-1 (TIMP-1)/β-actin (1:1000; Santa Cruz, USA). Each antigen-antibody complex was visualized using ECL Western blotting detection reagents and detected by chemiluminescence with Sensi-Q 2000 Chemidoc (Lugen Sci Co., Ltd., Gyeonggi-do, Korea). Band densities were measured using ATTO Densitograph Software (ATTO Corporation, Tokyo, Japan) and quantified as the ratio to histone or β-actin. The protein levels of the groups are expressed relative to those of the normal rat (represented as 1).

Statistical analysis

Data are expressed as mean ± standard error of the mean Statistical comparisons were assessed by one-way ANOVA followed by least-significant differences test (SPSS 22.0 for Windows, SPSS Inc., NY, USA). Values of $P < 0.05$ were considered significant.

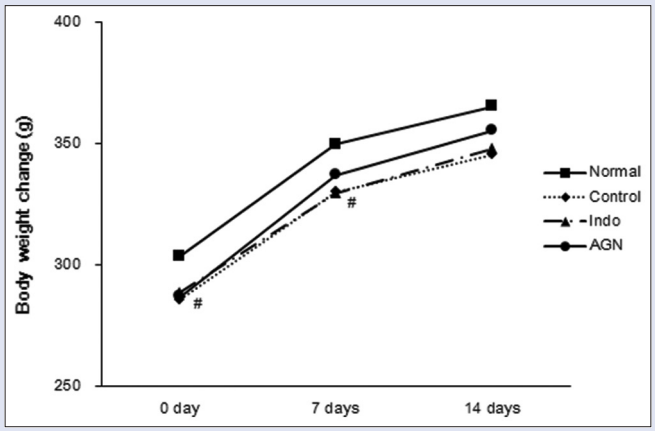

Figure 2: Body weight changes for 2 weeks. Values are the mean ± standard error of the mean ($n = 8$). Normal; Normal rats, Control; MIA-induced osteoarthritis rats, Indo; monosodium iodoacetate -induced osteoarthritis rats administrated with indomethacin 5 mg/kg body weight, *Angelica gigas* Nakai; monosodium iodoacetate -induced osteoarthritis rats administrated with *Angelica gigas* Nakai 200 mg/kg body weight. Significance: #$P < 0.05$ versus normal rat values

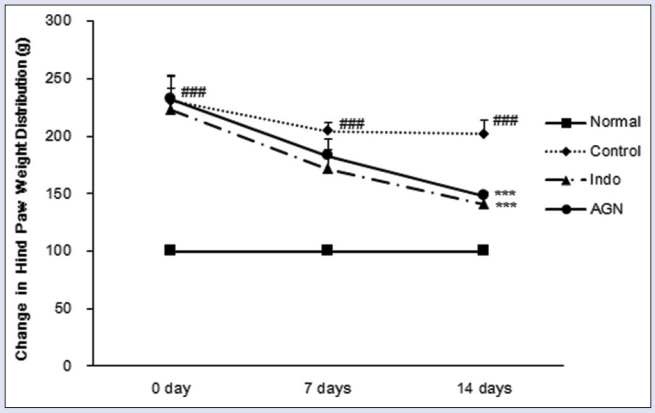

Figure 3: Change in hind paw weight distribution. Values are the mean ± standard error of the mean (n = 8). Normal; normal rats, control; monosodium iodoacetate-induced osteoarthritis rats, Indo; monosodium iodoacetate -induced osteoarthritis rats administrated with indomethacin 5 mg/kg body weight, *Angelica gigas* Nakai; monosodium iodoacetate -induced osteoarthritis rats administrated with *Angelica gigas* Nakai 200 mg/kg body weight. Significance: ###P < 0.001 versus Normal rat values and ***P < 0.001 versus monosodium iodoacetate control rat values

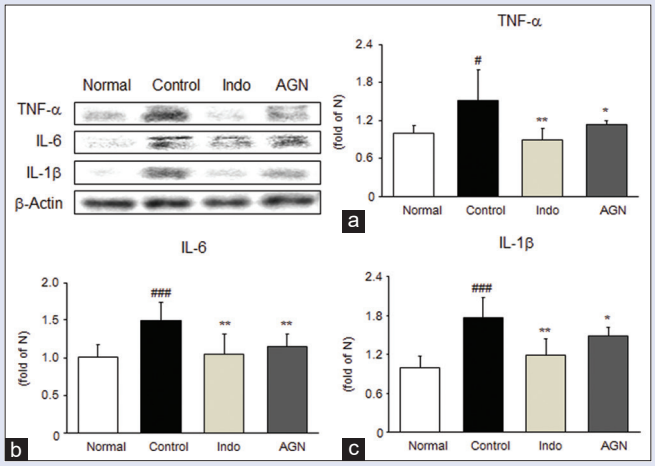

Figure 4: Tumor necrosis factor-α, interleukin-6 and interleukin-1β protein expressions in cartilaginous tissue. (a) Tumor necrosis factor-α, (b) interleukin-6 and (c) interleukin-1β. Values are the mean ± standard error of the mean (n = 8). Normal; normal rats, Control; monosodium iodoacetate induced osteoarthritis rats, Indo; monosodium iodoacetate -induced osteoarthritis rats administrated with indomethacin 5 mg/kg body weight, *Angelica gigas* Nakai; monosodium iodoacetate -induced osteoarthritis rats administrated with *Angelica gigas* Nakai 200 mg/kg body weight. Significance: #P < 0.05, ###P < 0.001 versus Normal rat values and *P < 0.05, **P < 0.01 versus monosodium iodoacetate control rat values

RESULTS

Body weight changes

Figure 2 shows the change in body weights during the experimental period. The groups, which were injected with MIA, displayed a lower body weight compared with normal group (P < 0.05). But there is no significance between each groups because of short experimental period.

Change hindpaw weight-bearing distribution

Hindpaw weight bearing distribution (HWBD), as a measure of OA progression, was measured as the difference between MIA-injected and contralateral hind limbs. The pain of knee joint leads to increase of HWBD, which has been proved for several study.[25] The HWBD on 0, 7 and 14 days is summarized in Figure 3. On day 0, MIA-treated group and AGN-treated group showed higher HWBD compared with normal group (P < 0.001). After 2 weeks, the increased HWBD was decreased at MIA-treated all experimental groups. Especially, when AGN-treated group improved significantly compared with MIA control group (P < 0.001). These results demonstrate a balance and relief of joint discomfort in the AGN-treated group.

Tumor necrosis factor-α, interleukin-6, and interleukin-1β in cartilaginous tissue

Figure 4 displayed the effect of AGN on the expression of inflammation-related cytokines, such as TNF-α, IL-6, and IL-1β. The MIA treatment significantly augmented the expressions of these cytokines (P < 0.05, P < 0.001). On the other hand, those expressions in Indo and AGN-treated groups were significantly decreased (P < 0.05, P < 0.01).

Matrix metalloproteinase-1 and tissue inhibitor of metalloproteinase-1 in cartilaginous tissue

Western bolt revealed that MIA treatment increased MMP-1 protein expression (P < 0.01). By contrast, TIMP-1 protein expression decreased (P < 0.05). On the other hand, AGN decreases MMP and increases TIMP-1 expression levels in cartilaginous tissue (P < 0.05, P < 0.01) [Figure 5].

p-IκBα and nuclear factor kappa B p65 in cartilaginous tissue

NF-κB activity of nuclear fraction and p-IκBα of cytosol fraction from cartilaginous tissue were analyzed by western blotting. Figure 6 indicated the effect of AGN. As expected, a significant elevation of NF-κB and p-IκBα activity were observed in MIA control group (P < 0.05, P < 0.001). Both NF-κB and p-IκBα activity were inhibited by AGN (P < 0.05, P < 0.01).

Inducible nitric oxide synthase and cyclooxygenase-2 in cartilaginous tissue

Figure 7 displayed the effect of AGN on the expression of inflammation-related mediators such as iNOS and COX-2. The MIA treatment significantly augmented the expressions of iNOS and COX-2 (P < 0.01). On the other hand, iNOS expression shows a decreasing tendency without a significance. Besides, COX-2 expression in AGN-treated group was significantly decreased (P < 0.05).

ROS and $ONOO^-$ in cartilaginous tissue

Figure 8 shows the effect of AGN on ROS and $ONOO^-$ level in cartilaginous tissue. The ROS level of MIA control group was significantly elevated to 197141 fluorescence/min/mg in comparison with that of normal group, at 94644 fluorescence/min/mg [Figure 3a]. On the other hand, it was significantly ameliorated by the administration of AGN, at 86737 fluorescence/min/mg (P < 0.01). The level of $ONOO^-$ was also increased by MIA treatment, whereas it was markedly reduced by AGN administration [Figure 3b, P < 0.01].

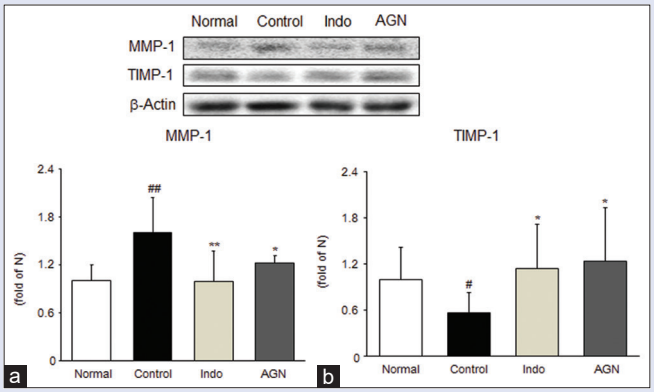

Figure 5: Matrix metalloproteinase-1 and tissue inhibitor of metalloproteinase-1 protein expressions in cartilaginous tissue. (a) Matrix metalloproteinase-1 and (b) tissue inhibitor of metalloproteinase-1. Values are the mean ± standard error of the mean ($n = 8$). Normal; normal rats, Control; monosodium iodoacetate-induced osteoarthritis rats, Indo; monosodium iodoacetate -induced osteoarthritis rats administrated with indomethacin 5 mg/kg body weight, *Angelica gigas* Nakai; monosodium iodoacetate -induced osteoarthritis rats administrated with *Angelica gigas* Nakai 200 mg/kg body weight. Significance: #$P < 0.05$, ##$P < 0.01$ versus normal rat values and *$P < 0.05$, **$P < 0.01$ versus monosodium iodoacetate control rat values

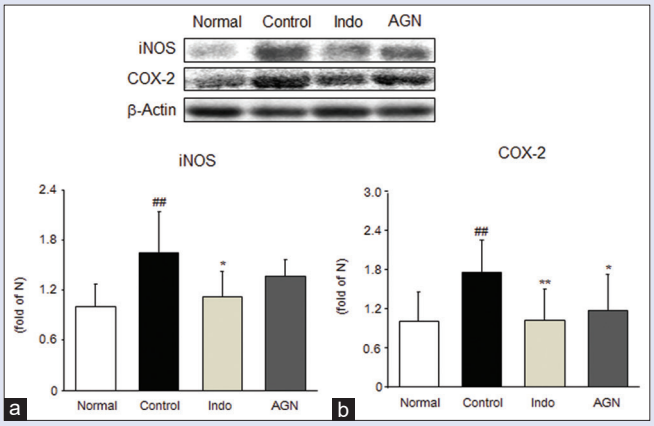

Figure 7: Inducible nitric oxide synthase and cyclooxygenase-2 protein expressions in cartilaginous tissue. (a) Inducible nitric oxide synthase and (b) cyclooxygenase-2 Values are the mean ± standard error of the mean ($n = 8$). Normal; normal rats, Control; monosodium iodoacetate -induced osteoarthritis rats, Indo; monosodium iodoacetate -induced osteoarthritis rats administrated with indomethacin 5 mg/kg body weight, *Angelica gigas* Nakai; monosodium iodoacetate -induced osteoarthritis rats administrated with *Angelica gigas* Nakai 200 mg/kg body weight. Significance: ##$P < 0.01$ versus normal rat values and *$P < 0.05$, **$P < 0.01$ versus monosodium iodoacetate control rat values

Nuclear factor erythroid 2-related factor 2/heme oxygenase-1 pathway in cartilaginous tissue

As shown in Figure 9, the Nrf2 protein expression was decreased in MIA control group as compared with normal group, whereas AGN treatment significantly upregulated ($P < 0.05$). Moreover, decreased HO-1 level by MIA treatment was significantly increased by AGN administration ($P < 0.05$, $P < 0.01$).

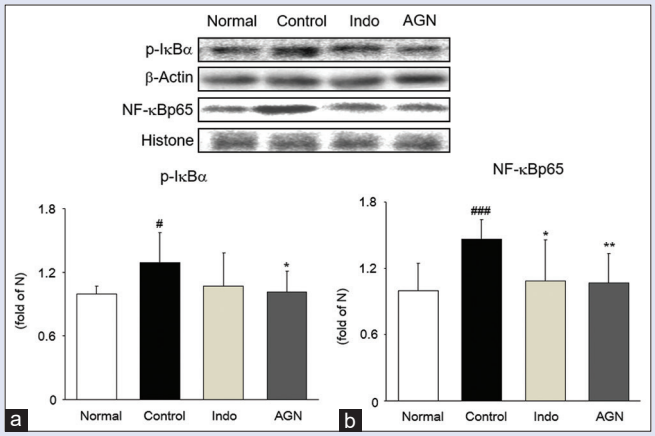

Figure 6: p-IκBα and nuclear factor kappa B p65 protein expressions in cartilaginous tissue. (a) p-IκBα and (b) nuclear factor kappa B p65. Values are the mean ± standard error of the mean ($n = 8$). Normal; normal rats, Control; monosodium iodoacetate-induced osteoarthritis rats, Indo; monosodium iodoacetate -induced osteoarthritis rats administrated with indomethacin 5 mg/kg body weight, *Angelica gigas* Nakai; monosodium iodoacetate -induced osteoarthritis rats administrated with *Angelica gigas* Nakai 200 mg/kg body weight. Significance: #$P < 0.05$, ###$P < 0.001$ versus normal rat values and *$P < 0.05$, **$P < 0.01$ versus monosodium iodoacetate control rat values

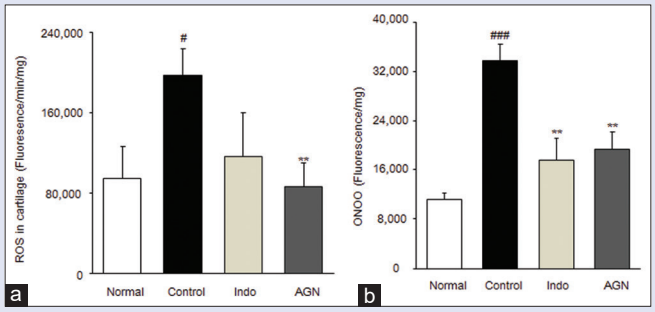

Figure 8: Effect of *Angelica gigas* Nakai on monosodium iodoacetate induced ROS and $ONOO^-$ formation in cartilaginous tissue. (a) ROS and (b) $ONOO^-$. Values are the mean ± standard error of the mean ($n = 8$). Normal; normal rats, Control; monosodium iodoacetate -induced osteoarthritis rats, Indo; monosodium iodoacetate -induced osteoarthritis rats administrated with indomethacin 5 mg/kg body weight, *Angelica gigas* Nakai; monosodium iodoacetate -induced osteoarthritis rats administrated with *Angelica gigas* Nakai 200 mg/kg body weight. Significance: #$P < 0.05$, ###$P < 0.001$ versus normal rat values and **$P < 0.01$ versus monosodium iodoacetate control rat values

DISCUSSION

AGN as herbal medicine has long been utilized and contains bioactive substances such as decursin (D), decursinol angelate (DA), nodakenin, demethylsuberosine, and decursinol (DOH). It is a well-studied pyranocoumarins with various pharmacological activities in cancer and inflammation.[26,27] Among pyranocoumarins, major compounds are D and DA. In addition, they are abundantly present in AGN.[28,29] After, the dried herb AGN (300 g) was extracted with distilled water (3 L) for 2 h, and it was named AGN. Our HPLC analysis also revealed a similar result [Figure 1]. AGN including these effective compounds may exert

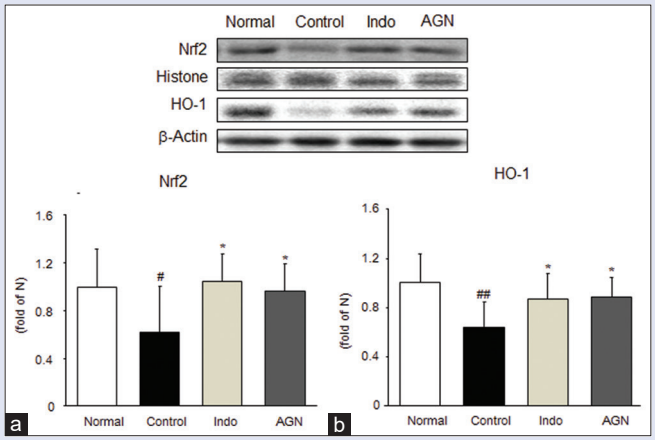

Figure 9: Nuclear factor erythroid 2-related factor 2 and heme oxygenase-1 protein expressions in cartilaginous tissue. (a) Nuclear factor erythroid 2-related factor 2 and (b) Heme oxygenase-1. Values are the mean ± standard error of the mean (n = 8). Normal; Normal rats, Control; monosodium iodoacetate -induced osteoarthritis rats, Indo; monosodium iodoacetate -induced osteoarthritis rats administrated with indomethacin 5 mg/kg body weight, *Angelica gigas* Nakai; monosodium iodoacetate -induced osteoarthritis rats administrated with *Angelica gigas* Nakai 200 mg/kg body weight. Significance: #P < 0.05, ##P < 0.01 versus normal rat values and *P < 0.05 versus monosodium iodoacetate control rat values

potential protective effects against OA. OA, which is characterized by chronic and degenerative joint disease, is the most common and prevalent type of arthritis.[30] The typical progression of OA causes pain and a substantial disability. The standard drugs available for the management of OA, such as NSAIDs, intraarticular corticosteroids, and cartilage protective agents can only relieve the clinical symptoms.[3] Another field of recent research is the efficacy of TNF-α blockers but anti-TNF-α agents are too expensive and also have various side effects.[31] So, new therapeutic approaches are needed. The present study was designed to explore the protective effect and possible underlying mechanism of AGN on a MIA-induced model of OA. The intra-articular injection of MIA, the chondrocyte glycolysis inhibitor is the common way to induce the OA chemically.[25,32] Specifically, we observed changes in HWBD and levels of antioxidant and inflammatory factors in serum or cartilaginous tissue. Both inflammatory factors such as cytokines and mediators have been implicated in OA pathogenesis.[33]

Many studies have been demonstrated inflammatory cytokines included IL-1 β, IL-6, and TNF-α are critical roles in OA pathogenesis,[34,35] which is intimately related to degradation of the ECM. Higher levels of these cytokines in the initiation and progression of articular cartilage destruction have been shown to correlate with pain and physical function of patients with OA.[36-38] In this study, the authors measured the IL-1 β, IL-6, and TNF-α expression levels within cartilage tissues in the MIA-induced OA model. The AGN treatment group showed a reduction of three cytokines production, especially, IL-6, inducing the production of acute-phase response proteins, reduced significantly. Pro-inflammatory cytokines are believed to cause cartilage damage including ECM degradation and several enzymes play important roles in this course; of these enzymes, matrix metalloproteinases (MMPs) and tissue inhibitor of metalloproteinases (TIMPs) have been diversely studied.[39] MMPs have been reported to degrade ECM alone or in combination with factors to facilitate the migration of inflammatory cells, whereas TIMPs inhibit MMP-induced ECM degradation to maintain normal homeostasis.[40] Therefore, excessive activation of MMPs increases tissue degradation. Hence, the balance between MMPs and TIMPs has to be well regulated to optimize ECM remodeling.[11] Our results in this study revealed that AGN suppresses the expression of MMP-1 and elevates TIMP-1, on MIA-induced OA.

A crucial cytokine-induced initiation of transcription is seen in the NF-κB signaling pathway. Inactivated NF-κB pathway, phosphorylation of IKKα/β and NF-κBp65 mediates the regulation of promoter activity of both anabolic and catabolic genes. NF-κB can influence the expression of inflammatory mediators such as iNOS and COX-2.[41] COX is a key pro-inflammatory enzyme that converts arachidonic acid into prostaglandins. Inhibition of NF-κB activation is associated with the down-regulation of COX-2 expression and synthesis. Moreover, the excessive iNOS induces the overproduction of NO. NO generates $ONOO^-$ through reacting with O_2^- and this can accelerate OA.[42] The results of the present study show that AGN promotes the suppression of NF-κB activation in cartilaginous tissue. As the result, the elevated expressions of COX-2 and iNOS were markedly attenuated by AGN treatment.

Oxidative stress (OS) is correlated with a reduction of antioxidant defenses and an increase in the production of ROS. Several studies have reported antioxidant activities of AGN.[13,43] Through this property, AGN might also protect against tissue damage in a cartilaginous tissue by regulating free radicals/ROS. The Nrf2 antioxidant pathway has been suggested as an important therapeutic target against OS. HO-1, a stress-responsive protein shortly activated by OA, has been known as the cytoprotective effect resistant to OA.[44] Herein, ROS were suppressed in AGN-treated group. In addition, our results revealed that AGN enhanced the ability of Nrf2 to migrate into the nucleus and activated the up-regulation of HO-1 expression through stimulation of Nrf2. As the result, AGN protected cartilaginous tissue from OS.

CONCLUSION

Taken together, it suggests that AGN could suppress excessive production of ROS and elevate antioxidant effect through Nrf2/HO-1 pathway. Moreover, AGN could inhibit the expression of inflammation factors by NF-κB inactivation. As the result, AGN treatment may have the potential therapeutic ability in the treatment of OA. However, the complete molecular mechanism of AGN has not been fully elucidated. Further research on AGN in humans is required before treatments after that AGN can be used safely in the clinic.

Financial support and sponsorship

This research was supported by the National Research Foundation of Korea (NRF) grant funded by the Korean government (MSIT) (No. 2018R1A5A2025272) and '2019 Development of Technology on Bio MediFood Using Medicinal Crop' funded by Gyeongsangbuk-do and Gyeongsan-si.

Conflicts of interest

There are no conflicts of interest.

REFERENCES

1. French HP, Galvin R, Horgan NF, Kenny RA. Prevalence and burden of osteoarthritis amongst older people in Ireland: Findings from The Irish LongituDinal Study on Ageing (TILDA). Eur J Public Health 2016;26:192-8.
2. Liu FC, Wang CC, Lu JW, Lee CH, Chen SC, Ho YJ, *et al.* Chondroprotective Effects of Genistein against Osteoarthritis Induced Joint Inflammation. Nutrients 2019;11:1180.
3. de Rezende MU, Gobbi RG. Drug therapy in knee osteoarthrosis. Rev Bras Ortop 2009;44:14-9.
4. Shakibaei M, John T, Schulze-Tanzil G, Lehmann I, Mobasheri A. Suppression of NF-kappaB activation by curcumin leads to inhibition of expression of cyclo-oxygenase-2 and matrix

metalloproteinase-9 in human articular chondrocytes: Implications for the treatment of osteoarthritis. Biochem Pharmacol 2007;73:1434-45.

5. Fernandes JC, Martel-Pelletier J, Pelletier JP. The role of cytokines in osteoarthritis pathophysiology. Biorheology 2002;39:237-46.
6. Calich AL, Domiciano DS, Fuller R. Osteoarthritis: can anti-cytokine therapy play a role in treatment? Clin Rheumatol 2010;29:451-5.
7. Kobayashi M, Squires GR, Mousa A, Tanzer M, Zukor DJ, Antoniou J, *et al.* Role of interleukin-1 and tumor necrosis factor alpha in matrix degradation of human osteoarthritic cartilage. Arthritis Rheum 2005;52:128-35.
8. Kapoor M, Martel-Pelletier J, Lajeunesse D, Pelletier JP, Fahmi H. Role of proinflammatory cytokines in the pathophysiology of osteoarthritis. Nat Rev Rheumatol 2011;7:33-42.
9. Zheng W, Zhang H, Jin Y, Wang Q, Chen L, Feng Z, *et al.* Butein inhibits IL-1β-induced inflammatory response in human osteoarthritis chondrocytes and slows the progression of osteoarthritis in mice. Int Immunopharmacol 2017;42:1-10.
10. Zeng GQ, Chen AB, Li W, Song JH, Gao CY. High MMP-1, MMP-2, and MMP-9 protein levels in osteoarthritis. Genet Mol Res 2015;14:14811-22.
11. Wakamatsu K, Nanki T, Miyasaka N, Umezawa K, Kubota T. Effect of a small molecule inhibitor of nuclear factor-kappaB nuclear translocation in a murine model of arthritis and cultured human synovial cells. Arthritis Res Ther 2005;7:R1348-59.
12. Rigoglou S, Papavassiliou AG. The NF-κB signalling pathway in osteoarthritis. Int J Biochem Cell Biol 2013;45:2580-4.
13. Azad MO, Piao JP, Park CH, Cho DH. Far infrared irradiation enhances nutraceutical compounds and antioxidant properties in *Angelica gigas* Nakai powder. Antioxidants (Basel) 2018;7:189.
14. Ok S, Oh SR, Jung TS, Jeon SO, Jung JW, Ryu DS. Effects of *Angelica gigas* Nakai as an anti-inflammatory agent in *in vitro* and *in vivo* atopic dermatitis models. Evid Based Complement Alternat Med 2018;2018:2450712.
15. Sowndhararajan K, Kim S. Neuroprotective and cognitive enhancement potentials of *Angelica gigas* Nakai root: A Review. Sci Pharm 2017;85:21.
16. Reddy CS, Kim SC, Hur M, Kim YB, Park CG, Lee WM, *et al.* Natural korean medicine dang-gui: Biosynthesis, effective extraction and formulations of major active pyranocoumarins, their molecular action mechanism in cancer, and other biological activities. Molecules 2017;22:2170.
17. Islam SU, Lee JH, Shehzad A, Ahn EM, Lee YM, Lee YS. Decursinol angelate inhibits LPS-induced macrophage polarization through modulation of the NFκB and MAPK signaling pathways. Molecules 2018;23:1880.
18. Shehzad A, Parveen S, Qureshi M, Subhan F, Lee YS. Decursin and decursinol angelate: Molecular mechanism and therapeutic potential in inflammatory diseases. Inflamm Res 2018;67:209-18.
19. Kim JH, Jeong JH, Jeon ST, Kim H, Ock J, Suk K, *et al.* Decursin inhibits induction of inflammatory mediators by blocking nuclear factor-kappaB activation in macrophages. Mol Pharmacol 2006;69:1783-90.
20. Wang ZM, Zhu SG, Wu ZW, Lu Y, Fu HZ, Qian RQ. Kirenol upregulates nuclear annexin-1 which interacts with NF-κB to attenuate synovial inflammation of collagen-induced arthritis in rats. J Ethnopharmacol 2011;137:774-82.
21. Chun JM, Lee AY, Kim JS, Choi G, Kim SH. Protective effects of *Peucedanum japonicum* extract against osteoarthritis in an animal model using a combined systems approach for compound-target prediction. Nutrients 2018;10:754.
22. Ali SF, LeBel CP, Bondy SC. Reactive oxygen species formation as a biomarker of methylmercury and trimethyltin neurotoxicity. Neurotoxicology 1992;13:637-48.
23. Kooy NW, Royall JA, Ischiropoulos H, Beckman JS. Peroxynitrite-mediated oxidation of dihydrorhodamine 123. Free Radic Biol Med 1994;16:149-56.
24. Komatsu S. Extraction of nuclear proteins. Methods Mol Biol 2007;355:73-7.
25. Kil JS, Kim MG, Choi HM, Lim JP, Boo Y, Kim EH, *et al.* Inhibitory effects of Angelicae Gigantis Radix on osteoclast formation. Phytother Res 2008;22:472-6.
26. Schuelert N, McDougall JJ. Grading of monosodium iodoacetate-induced osteoarthritis reveals a concentration-dependent sensitization of nociceptors in the knee joint of the rat. Neurosci Lett 2009;465:184-8.
27. Kim HJ, Lee GJ, Choi AJ, Kim TH, Kim TI, Oh JM. Layered double hydroxide nanomaterials encapsulating *Angelica gigas* Nakai extract for potential anticancer nanomedicine. Front Pharmacol 2018;9:723.
28. Lee HJ, Lee HJ, Lee EO, Lee JH, Lee KS, Kim KH, *et al. In vivo* anti-cancer activity of Korean *Angelica gigas* and its major pyranocoumarin decursin. Am J Chin Med 2009;37:127-42.
29. Cho SK, Abd El-Aty AM, Choi JH, Kim MR, Shim JH. Optimized conditions for the extraction of secondary volatile metabolites in Angelica roots by accelerated solvent extraction. J Pharm Biomed Anal 2007;44:1154-8.
30. Pereira D, Ramos E, Branco J. Osteoarthritis. Acta Med Port 2015;28:99-106.
31. Hermann W, Lambova S, Muller-Ladner U. Current treatment options for osteoarthritis. Curr Rheumatol Rev 2018;14:108-16.
32. Guzman RE, Evans MG, Bove S, Morenko B, Kilgore K. Mono-iodoacetate-induced histologic changes in subchondral bone and articular cartilage of rat femorotibial joints: An animal model of osteoarthritis. Toxicol Pathol 2003;31:619-24.
33. Wojdasiewicz P, Poniatowski ŁA, Szukiewicz D. The role of inflammatory and anti-inflammatory cytokines in the pathogenesis of osteoarthritis. Mediators Inflamm 2014;2014:561459.
34. Yan L, Zhou L, Xie D, Du W, Chen FM, Yuan Q, *et al.* Chondroprotective effects of platelet lysate towards monoiodoacetate-induced arthritis by suppression of TNF-α-induced activation of NF-κB pathway in chondrocytes. Aging 2019;11:2797-811.
35. Zhou K, Hu L, Liao W, Yin D, Rui F. Coptisine Prevented IL-β-induced expression of inflammatory mediators in chondrocytes. Inflammation 2016;39:1558-65.
36. Penninx BW, Abbas H, Ambrosius W, Nicklas BJ, Davis C, Messier SP, *et al.* Inflammatory markers and physical function among older adults with knee osteoarthritis. J Rheumatol 2004;31:2027-31.
37. Van de Loo FA, Joosten LA, van Lent PL, Arntz OJ, van den Berg WB. Role of interleukin-1, tumor necrosis factor α, and interleukin-6 in cartilage proteoglycan metabolism and destruction: Effect of *in situ* blocking in murine antigen- and zymosan-induced arthritis. Arthritis Rheum 1995;38:164-72.
38. Fuchs S, Skwara A, Bloch M, Dankbar B. Differential induction and regulation of matrix metalloproteinases in osteoarthritic tissue and fluid synovial fibroblasts. Osteoarthritis Cartilage 2004;12:409-18.
39. Kieseier BC, Schneider C, Clements JM, Gearing AJ, Gold R, Toyka KV, *et al.* Expression of specific matrix metalloproteinases in inflammatory myopathies. Brain 2001;124:341-51.
40. Alameddine HS. Matrix metalloproteinases in skeletal muscles: Friends or foes? Neurobiol Dis 2012;48:508-18.
41. Pan T, Chen R, Wu D, Cai N, Shi X, Li B, *et al.* Ipha-Mangostin suppresses interleukin-1β-induced apoptosis in rat chondrocytes by inhibiting the NF-κB signaling pathway and delays the progression of osteoarthritis in a rat model. Int Immunopharmacol 2017;52:156-62.
42. Tian B, Liu J, Bitterman PB, Bache RJ. Mechanisms of cytokine induced NO-mediated cardiac fibroblast apoptosis. Am J Physiol Heart Circ Physiol 2002;283:H1958-67.
43. Noh BY, Lee HJ, Do JR, Kim HK. Antioxidant and ACE inhibitory activity of cultivated and wild *Angelica gigas* Nakai extracts prepared using different extraction conditions. Prev Nutr Food Sci 2014;19:274-80.
44. Bae WJ, Ha US, Choi JB, Kim KS, Kim SJ, Cho HJ, *et al.* Protective effect of decursin extracted from *Angelica gigas* in male infertility via Nrf2/HO-1 signaling pathway. Oxid Med Cell Longev 2016;2016:5901098.